

Efficiency improvement of solar air collectors used in drying processes

DOI: 10.54598/006050

PhD Thesis

by

Machi Maytham Hasan Mahdi

Gödöllő 2025

Doctoral school	
Denomination:	Doctoral School of Mechanical Engineering
Science:	Mechanical Engineering
Leader:	Prof. Dr. Gábor Kalácska, DSc Institute of Technology Hungarian University of Agriculture and Life Sciences Gödöllő, Hungary
Supervisor:	Prof. Dr. István Farkas, DSc Institute of Technology Hungarian University of Agriculture and Life Sciences Gödöllő, Hungary
Co-Supervisor:	Dr. János Buzás, PhD Institute of Technology Hungarian University of Agriculture and Life Sciences, Gödöllő, Hungary
Affirmation	of supervisors Affirmation of head of school

CONTENTS

1.	INTRODUCTION, OBJECTIVES	4
2.	MATERIALS AND METHODS	5
	2.1. Description of the tested rigs	5
	2.2. Experimental setup and procedure	5
	2.2.1. Effect of entrance flue design	6
	2.2.2. Effect of V-angled fins design	6
	2.2.2.1. Continuous perforated V-angled fins	6
	2.2.2.2. Discrete perforated V-angled fins	7
	2.2.3. Impact of selective coatings	7
	2.2.4. Influence of channel depth	8
	2.2.5. Effect of different fin configurations on drying performance	8
3.	RESULTS	9
	3.1. Effect of entrance flue design evaluation	9
	3.2. Effect of V-angled fins design evaluation	10
	3.2.1. Continuous perforated V-angled fins evaluation	10
	3.2.2. Discrete perforated V-angled fins evaluation	11
	3.3. Impact of selective coatings evaluation	13
	3.4. Influence of channel depth evaluation	15
	3.4.1. Effect on single pass mode	15
	3.4.2. Effect on double pass mode	17
	3.5. Effect of different fins configuration on drying process	18
4.	NEW SCIENTIFIC RESULTS	20
5.	CONCLUSION AND SUGGESTIONS	24
6.	SUMMARY	25
7	MOST IMPORTANT PUBLICATIONS RELATED TO THE THESIS	26

1. INTRODUCTION, OBJECTIVES

Solar energy is harnessed using thermal collectors, which produce heat, and photovoltaic modules, which generate electricity. Among these, solar air collectors (SACs) are widely used for air heating and drying applications due to their simplicity and cost-effectiveness. However, challenges such as low heat transfer efficiency and elevated heat losses limit their performance.

Enhancing thermal energy transfer in SACs is crucial for optimizing their efficiency. Researchers have explored innovative design modifications, including adjustments to absorber surfaces and the use of various flow channel configurations (single, double, or triple pass). However, achieving a balance between these enhancements and their potential limitations remains a key challenge in advancing SAC technology.

A comprehensive review of experimental and theoretical studies has identified various factors influencing the performance of SACs. However, there remains a significant lack of experimental investigations to evaluate SACs performance, particularly regarding the effects of entrance flue conditions, channel height, selective coatings, and different absorber configurations on SAC efficiency

This research aims to bridge these gaps through extensive experimental analysis conducted outdoors. Four SAC prototypes were constructed, and experiments were performed on both single-pass (SPSAC) and double-pass (DPSAC) configurations. Novel V-angled fins with varying lengths and orientations were introduced and rigorously tested to improve heat transfer and thermal efficiency.

The primary objectives of this research are:

- To examines the effect of entrance flue conditions on the performance of single pass solar air collectors.
- To study experimentally the performance of double pass solar air collectors using different absorber configurations.
- To investigate and compare the effect of using selective coating on the performance of solar air collectors.
- To examine numerically and experimentally the effect of channel height on the performance of solar air collector.
- To study experimentally the influence of different fins configuration on drying process.

2. MATERIALS AND METHODS

This chapter offers a detailed description of the materials, methodologies, and equipment employed in the experimental investigations, along with the scientific frameworks adopted to fulfil the research objectives.

2.1. Description of the tested rigs

To achieve the study objectives, four SACs were constructed using locally available materials. Each SAC was uniquely modified for specific experimental purposes. These collectors comprised a wooden frame, an insulated base, a transparent plastic cover for optimal solar radiation transmittance, and a smooth copper absorber plate coated with black matte paint to enhance solar energy absorption.

Two single-pass solar air collectors (SPSACs) were built with wooden frames measuring $125 \times 50 \times 13$ cm, insulated with polystyrene sheets of 2 cm and 3 cm thickness. A smooth copper absorber plate with dimensions $121 \times 46 \times 1.2$ mm was installed, and the top surface was enclosed with a transparent plastic cover. This design created a 55 mm air passage between the absorber and the transparent cover to facilitate airflow and heat transfer.

Two double-pass solar air collectors (DPSACs) were constructed using similar materials and dimensions as the SPSACs, with a key modification of an additional air passage. A 35 mm lower air passage was added beneath the absorber plate, while the upper air passage remained 55 mm. Wooden buffers were strategically placed to guide airflow and improve distribution in the lower passage. Later, modifications were made to the absorber configurations to align with specific research objectives.

Additionally, two dehydration chambers were fabricated using extruded polystyrene insulation (XPS) sheets, designed for effective thermal insulation and ease of assembly. The dehydration chambers were designed as rectangular structures with internal dimensions of $52\times47\times100$ cm. Each chamber featured three sliding dehydration trays made of plastic netting, allowing for easy loading and unloading of materials. The chamber walls were opaque, except for the front, which was covered with a transparent material to allow sunlight penetration. An inclined roof enhanced airflow within the chamber, while air entered through an inlet below the door and exited via an outlet on the roof. The chambers were connected to the SACs through a 100 mm insulated piping system to facilitate the transfer of heated air. The structure layout of the SACs is detailed in Fig. 1

2.2. Experimental setup and procedure

This section outlines the experimental procedures used to achieve the research objectives. The same collectors were utilized across all experiments, with

specific modifications made for each experiment to align with the thesis objectives. Calibration, setup, and consistent data collection methods ensured validity and reproducibility.

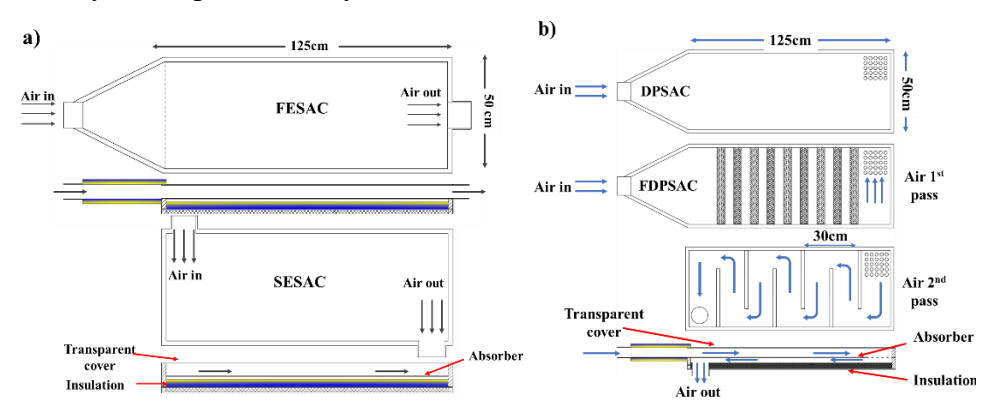


Fig. 1. The structure layout of the collectors: a) SPSAC, b) DPSAC

2.2.1. Effect of entrance flue design

This experiment evaluated the performance of two SPSACs: the front entrance solar air collector (FESAC) and the side entrance solar air collector (SESAC), under outdoor conditions. FESAC featured a rectangular air inlet (11 cm × 5.5 cm) positioned on the upper long side, with the outlet directly opposite on the lower side for efficient airflow. In contrast, SESAC included a divergent inlet (35 cm long, 46 cm wide at the base) to distribute air evenly across the absorber plate, enhancing air distribution and heat transfer efficiency. Both collectors were tested simultaneously to isolate the impact of their air entry designs on thermal performance. Precise assembly and calibration of components, including airflow ducts, thermocouples, and pressure sensors, ensured accuracy and minimized air leakage. Tests were conducted during clear August 2023 days, using mass flow rates (MFR) of 0.01118 kg/s (case A), 0.01231 kg/s (case B), and 0.01469 kg/s (case C). A variable-speed fan controlled and stabilized airflow. Data on temperatures from multiple sensors, pressure drops at the orifice plate, and solar radiation intensity were collected every minute and graphed at five-minute intervals.

2.2.2. Effect of V-angled fins design

2.2.2.1. Continuous perforated V-angled fins

This experiment investigated the impact of continuous V-angled perforated fins on the thermal performance of DPSACs. The tested collectors' materials and dimensions are detailed in the rigs fabrication section, with configurations shown in Fig. 1(b). The fins, each with a 90° angle and 2.5 cm sides, were placed at a 45° angle relative to the absorber plate, with 78 holes (39 of 8 mm

and 39 of 6 mm in diameter) distributed along their 45 cm length. Nine fins were installed, spaced 100 mm apart. The fins were securely attached using bolts and thermal silicone adhesive. Experiments compared two collectors: a smooth DPSAC and a finned FDPSAC, tested side by side under outdoor conditions to isolate the effects of the fin configuration. Both collectors were carefully assembled, sealed, and calibrated, ensuring consistent readings. Tests were conducted from August 15–22, 2023, at a MFRs of 0.00864 kg/s (case I), 0.01143 kg/s (case II), and 0.01317 kg/s (case III). Data on temperatures from multiple sensors, pressure drops at the orifice plate, and solar radiation intensity were collected every minute from 10:30 AM to 3:30 PM and graphed at five-minute intervals.

2.2.2.2. Discrete perforated V-angled fins

This experiment assessed the effect of discrete perforated V-angled fins on the thermal performance of SACs, using the same collectors and experimental methodology as the continuous fin tests. The discrete fins, with 6 cm sides and a 90° angle, were positioned at a 45° angle to the absorber surface. Each fin featured six 4 mm diameter holes, arranged systematically along its length. A total of 23 fins were installed in a staggered pattern, spaced 100 mm apart, and securely fastened using bolts and thermal adhesive for optimal heat transfer.

Three absorber configurations were tested: *Type I* (fins parallel to airflow), *Type II* (fins at a 45° angle to airflow), and *Type III* (fins perpendicular to airflow). These configurations, along with a smooth DPSAC, were tested side by side under outdoor conditions at three MFRs: 0.00932 kg/s, 0.01143 kg/s, and 0.01311 kg/s, between September 1 and 15, 2023. After each trial, the fin orientation was adjusted on the finned collectors, while the smooth collector remained unchanged. Data on temperatures from multiple sensors, pressure drops at the orifice plate, and solar radiation intensity were collected every minute from 10:30 AM to 3:30 PM and graphed at five-minute intervals.

2.2.3. Impact of selective coatings

In this experiment, two smooth DPSACs were tested to evaluate the effect of coatings on thermal performance. One was painted with regular black matte, and the other was coated with SOLKOTE HI/SORB-II selective coating, applied per the manufacturer's guidelines. Surface preparation included sanding with 120 and 240 disk sandpaper, degreasing with acetone, and applying five layers of coating with air atomization spray, followed by a two-week room-temperature cure. The DPSACs were tested side by side under outdoor conditions, ensuring proper assembly, sealing, and sensor calibration to minimize air leakage and ensure consistent measurements. The collectors were then converted into SPSACs to compare the selective coating's effects on both configurations. Testing covered a range of MFRs: SPSAC (0.00946, 0.01388, 0.02158, and 0.02629 kg/s) and DPSAC (0.00877, 0.01059, 0.01425,

and 0.01632 kg/s). Data on temperatures from multiple sensors, pressure drops at the orifice plate, and solar radiation intensity were collected every minute from 10:30 AM to 3:30 PM and graphed at five-minute intervals.

2.2.4. Influence of channel depth

The impact of channel depth on SAC performance was studied using experimental and mathematical methods. For the single-pass mode experiments, the SPSAC-5.5 cm (reference collector) was compared with SPSAC-7.5 cm and SPSAC-3.5 cm at modified channel depths (see Fig. 2). Tests were conducted at fixed MFRs, with SPSAC-7.5 cm tested at 0.00901 and 0.01527 kg/s, and SPSAC-3.5 cm at 0.00892 and 0.01813 kg/s. For double-pass mode, only the upper channel depth was varied using mathematical modeling. The model, validated against experimental data at 0.0103 kg/s, demonstrated good agreement. Simulations were then used to evaluate DPSAC performance at different channel depths.

2.2.5. Effect of different fin configurations on drying performance

To evaluate the performance enhancements of the proposed collector modifications, the drying process was used as a direct indicator of thermal efficiency. Experiments assessed the impact of various DPSAC fin configurations, including discrete V-angled fins ($Type\ II$: parallel to airflow, $Type\ II$: inclined at 45°, and $Type\ III$: perpendicular to airflow) and continuous V-angled fins ($Type\ IV$: perpendicular to airflow). A smooth absorber plate collector was tested as a baseline for comparison. Each chamber dehydrated 1200 grams of apple slices across three trays (400 ± 1 grams per tray), with slices cut to a uniform thickness of ~4 mm. Initial and hourly weights were recorded to monitor drying progress, with final weights noted at the experiment's conclusion. Experiments ran over several days at a fixed mass flow rate of 0.0103 kg/s, with a five-hour drying period from 10:30 AM to 3:30 PM. Key parameters were monitored and recorded throughout the process.

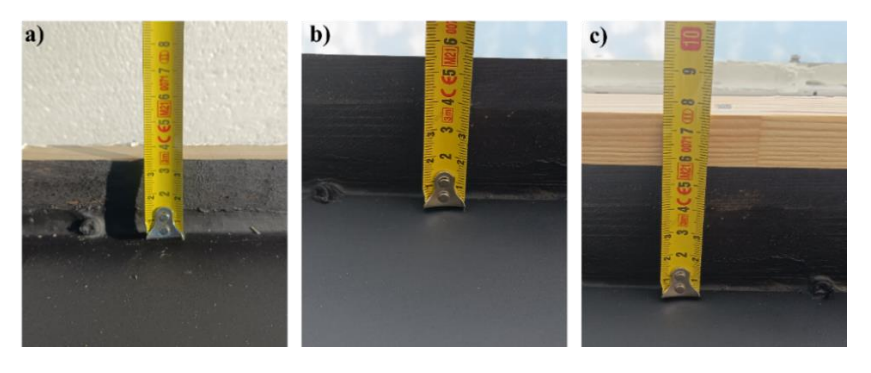


Fig. 2. SACs with varying channel depths: a) 3.5 cm, b) 5.5 cm, c) 7.5 cm

3. RESULTS

This chapter presents the most important results obtained from the experimentation and their discussions.

3.1. Effect of entrance flue design evaluation

The experiments, conducted in August 2023 at MATE University, Gödöllő, Hungary, assessed two solar air collectors with identical dimensions but different inlet designs. Both were tested simultaneously at three airflow rates to minimize weather-related variability and ensure reliable, valid results.

Fig. 3 compares outlet temperatures of the collectors over time for three airflow rate cases: 0.01118 kg/s (case A), 0.01231 kg/s (case B), and 0.01469 kg/s (case C). Both collectors show similar trends: temperatures rise in the morning, peak between 12:30 and 13:30, and decline in the afternoon as solar intensity decreases. However, FESAC consistently achieves higher outlet temperatures due to better air distribution, which enhances heat transfer. Maximum outlet temperatures for FESAC were 45.2 °C, 42.9 °C, and 39.5 °C, compared to SESAC's 43.1 °C, 41.4 °C, and 37.8 °C. The results show that increasing airflow reduces outlet temperatures, with FESAC maintaining superior performance due to its optimized design.

Fig. 4 illustrates the heat gain rate of the SACs, influenced by outlet temperature, solar radiation, and mass flow rate. Heat gain rate trends closely follow solar radiation curves, with airflow rate playing a dominant role. The useful heat increases primarily due to higher airflow rates and rising outlet temperatures. FESAC consistently outperformed SESAC, achieving maximum heat gain rate of 229.4 W, 240 W, and 277.8 W for the three airflow rates, compared to SESAC's 215.7 W, 230.1 W, and 257.8 W under the same conditions. This demonstrates FESAC's superior design and efficiency.

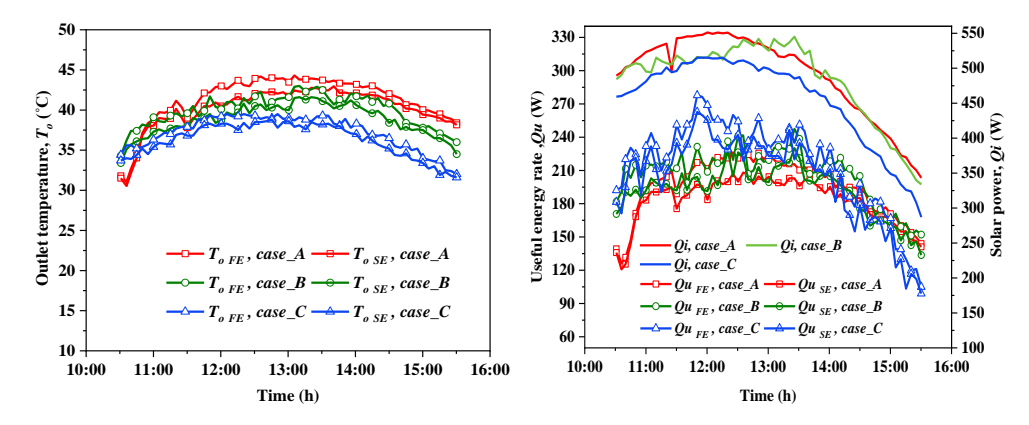


Fig. 3. Outlet temperature profiles for the collectors over time

Fig. 4. The useful energy rate by the collectors over time

Fig. 5 presents the instantaneous thermal efficiency trends for tested collectors at different MFRs. As illustrated, the FESAC achieved higher maximum efficiencies of 43.8%, 47.3%, and 53.9% for cases *A*, *B*, and *C*, compared to SESAC's 41.6%, 44.7%, and 51.1%. While FESAC consistently outperformed SESAC, instantaneous efficiency alone may not fully represent collector performance.

Efficiency calculations on an hourly or daily basis, as shown in Fig. 6, provide a more accurate evaluation. Daily efficiency was calculated by integrating instantaneous values. Results showed FESAC consistently outperformed SESAC, with daily efficiencies of 39.9%, 43.4%, and 47.5% at airflow rates of 0.01118 kg/s, 0.01231 kg/s, and 0.01469 kg/s, respectively, compared to SESAC's 37.2%, 40.4%, and 44.4%. The 6.9%–7.4% relative efficiency improvement in FESAC is primarily attributed to its front entrance design.

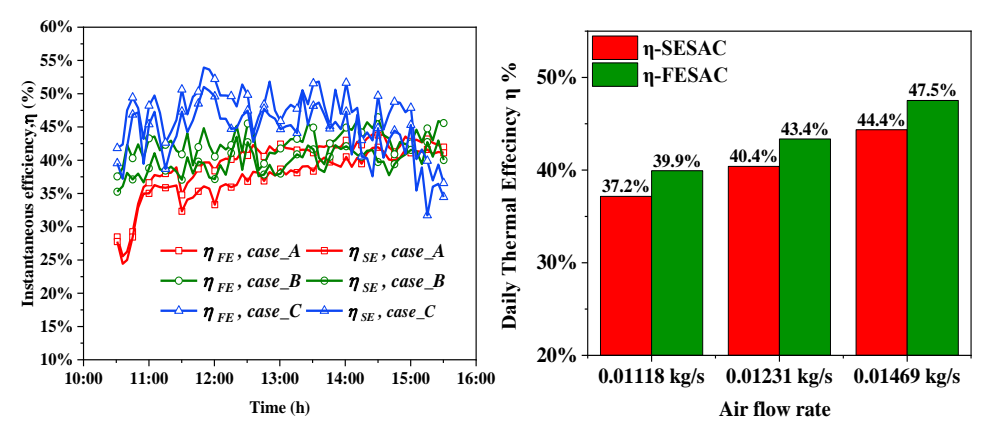


Fig. 5. Instantaneous thermal efficiency over time

Fig. 6. Comparing the daily efficiency versus MFRs

3.2. Effect of V-angled fins design evaluation

3.2.1. Continuous perforated V-angled fins evaluation

This section presents the performance evaluation of smooth (DPSAC) and continuous perforated V-angled finned (FDPSAC) collectors, tested outdoors from August 15–22, 2023, under clear conditions. Experiments followed rigorous procedures, with both collectors tested side-by-side at airflow rates of 0.00864 kg/s (*case II*), 0.01143 kg/s (*case III*), and 0.01317 kg/s (*case III*). This setup minimized external influences, ensuring a focused comparison of the designs. Data analysis includes temperature measurements, pressure drops, and solar radiation to evaluate thermal efficiency and heat transfer performance. Fig. 7 shows the variation in outlet temperature (T_o) for each flow rate. The T_o follows solar radiation patterns, rising in the morning, peaking at noon, and declining by 15:30. An inverse relationship is observed,

with T_o decreasing as airflow increases. The maximum T_o for FDPSAC was 60.6 °C, 57 °C, and 56.2 °C for cases I, II, and III, compared to DPSAC's 59 °C, 55 °C, and 53 °C. FDPSAC consistently achieved higher T_o due to its V-angled fins, which enhance heat transfer by increasing surface area and disrupting stagnant air layers. Fig. 8 illustrates the energy gain rate profiles, which rise from mid-morning, peak at noon, and decline, aligning with the solar power energy curve (Qi). Energy gain rate is influenced by flow rate and temperature difference (ΔT), with FDPSAC outperforming DPSAC in all cases. FDPSAC recorded maximum energy rate of 267.1 W, 297.3 W, and 318.3 W for cases I, II, and III, compared to DPSAC's 256.5 W, 274.4 W, and 289 W. These results confirm the superior performance of FDPSAC.

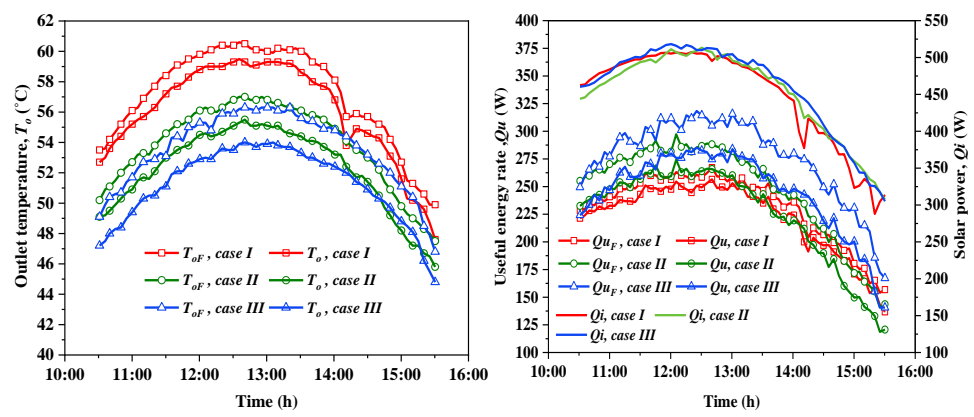


Fig. 7. Outlet temperature profiles for the collectors over time

Fig. 8. Energy gain rate by the collectors over time

Fig. 9 presents the instantaneous thermal efficiency trends for tested collectors at different MFRs. The trend shows FDPSAC achieving higher instantaneous efficiencies of 58.2%, 59.4%, and 64.8% for cases *I*, *II*, and *III*, compared to DPSAC's 54.7%, 54.8%, and 57%. Instantaneous efficiency, sensitive to solar radiation, highlights the need for daily efficiency calculations for accurate evaluation. Daily efficiencies, calculated using the trapezoidal rule, confirm FDPSAC's superiority. Fig. 10 shows daily efficiencies of 51.6%, 54.7%, and 59.2% for FDPSAC at flow rates of 0.00864 kg/s, 0.01143 kg/s, and 0.01317 kg/s, compared to DPSAC's 49.4%, 50.5%, and 53.9%. The continuous V-angled perforated fins relatively improved FDPSAC daily efficiency by 4.45–9.83% over DPSAC, validating the design's effectiveness and confirming its enhanced performance at higher flow rates.

3.2.2. Discrete perforated V-angled fins evaluation

This section presents the results of experiments evaluating the impact of discrete perforated V-angled fins on DPSAC thermal performance. Using the same setup and methodology as for continuous fins, three configurations were tested: *Type I* (parallel to airflow), *Type II* (inclined at 45°), and *Type III*

(perpendicular to airflow), alongside a smooth DPSAC. Experiments were conducted outdoors at MFRs of 0.00932, 0.01143, and 0.01311 kg/s. Data on temperatures, pressure drops, and solar radiation were collected to analyse the influence of fin orientation on heat transfer and overall performance.

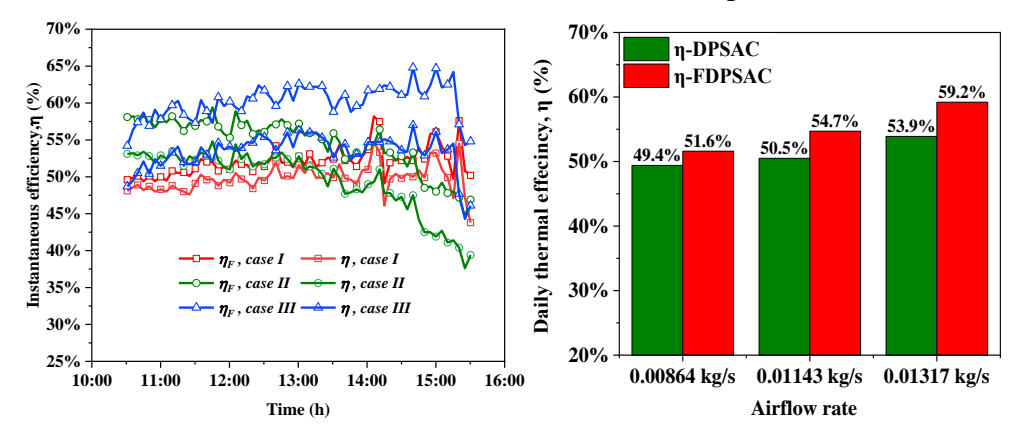


Fig. 9. Instantaneous thermal efficiency over time

Fig. 10. Comparing the daily efficiency versus MFRs

For Type I, maximum T_o values were 57 °C, 53.1 °C, and 50.8 °C for MFRs of 0.00932, 0.01143, and 0.01311 kg/s, slightly higher than the smooth collector, which reached 56.1 °C, 52 °C, and 49.6 °C under identical conditions. The parallel fins expanded the heat transfer area but generated limited turbulence, reducing their effectiveness compared to inclined orientations. The Type II recorded the highest T_0 at 58.5 °C, 55 °C, and 51.6 °C for the same MFRs, compared to smooth one which reached 54.8 °C, 51.2 °C, and 49.3 °C. Its V-angle and perforations created secondary flows and localized jets, disrupting the boundary layer and enhancing heat transfer, outperforming all configurations. The Type III reached T_o values of 56.2 °C, 54.4 °C, and 50.4 °C, showing moderate gains compared to the smooth collector, which recorded values of 55.1 °C, 53.1 °C, and 48.9 °C. Its perpendicular fins expanded the surface area and introduced moderate turbulence, though less effectively than Type II. These results confirm that Type II fins, with their optimized surface area, turbulence generation achieve superior thermal performance. The inverse relationship between MFR and T_o underscores the importance of balancing flow rate to optimize heat extraction without sacrificing efficiency.

The results showed that daily efficiency of the finned collectors consistently outperforming smooth collectors across all MFRs. The *Type I* fins achieved efficiencies of 52.5%, 54.9%, and 56.9% at MFRs of 0.00932 kg/s, 0.01143 kg/s, and 0.01311 kg/s, compared to 50.4%, 52.3%, and 54.1% for smooth collectors. The *Type II* fins demonstrated the highest efficiencies, achieving

53.6%, 56.9%, and 60.7%, surpassing the corresponding efficiencies of the DPSAC at 50.6%, 52.7%, and 55.6%. Similarly, the *Type III* fins recorded efficiencies of 53.3%, 55.8%, and 58.7%, outperforming the smooth collector, which achieved 51.1%, 53.1%, and 55.3%. The *Type II* fins consistently provided the highest efficiency, followed by *Type III* and *Type I*. Efficiency relative improvements ranged from 4.1% to 9.1%, with *Type II* delivering the greatest gains. These results highlight the effectiveness of perforated discrete V-angled fins in enhancing heat transfer and optimizing solar collector performance.

3.3. Impact of selective coatings evaluation

This section presents experimental findings on the impact of selective coatings on the thermal performance of SACs for both single-pass and double-pass configurations. Two identical collectors, one coated with SOLKOTE HI/SORB-II (Se) and the other with standard black matte (Bl), were tested under identical outdoor conditions across various MFRs to assess thermal efficiency, temperature differentials, and heat transfer rates. The SPSAC tests used MFRs of 0.00946 kg/s, 0.01388 kg/s, 0.02158 kg/s, and 0.02629 kg/s, while DPSAC tests used 0.00877 kg/s, 0.01059 kg/s, 0.01425 kg/s, and 0.01632 kg/s.

Fig. 11 shows T_o profiles for various MFRs in single-pass and double-pass modes. The T_o rises in the morning with increasing solar radiation, peaks between 11:30 and 12:30, and then gradually declines. Higher MFRs result in lower T_o . In single-pass mode, SPSAC-Se consistently achieved higher T_o than SPSAC-Bl. At the highest flow rate (0.02629 kg/s), maximum T_o was 42.5 °C for SPSAC-Se and 41.6 °C for SPSAC-Bl, while at the lowest flow rate (0.00946 kg/s), To reached 50.4 °C and 49.5 °C, respectively. Intermediate flow rates showed similar trends, with SPSAC-Se recording slightly higher temperatures. In double-pass mode, DPSAC-Se also outperformed DPSAC-Bl, particularly at lower flow rates. At 0.01632 kg/s, To was 50.4 °C for DPSAC-Se and 49.3 °C for DPSAC-Bl. At the lowest flow rate (0.00877 kg/s), T_o was 58.6 °C for DPSAC-Se compared to 57.7 °C for DPSAC-Bl. These results highlight the significant thermal performance improvement from selective coatings, particularly at lower flow rates, due to enhanced absorptivity and reduced radiative losses, improving heat retention and efficiency in SACs.

Fig. 12 shows absorber plate temperature variations for different MFRs in single-pass and double-pass modes. Temperatures rise with solar radiation in the morning, peak around midday, and decline in the afternoon, consistent across all configurations and MFRs. In single-pass mode, SPSAC-Se recorded maximum absorber temperatures of 90.5 °C, 84.1 °C, 76.4 °C, and 75.3 °C at MFRs of 0.00946 kg/s, 0.01388 kg/s, 0.02158 kg/s, and 0.02629 kg/s,

compared to SPSAC-Bl's 84.6 °C, 78.8 °C, 72.3 °C, and 70.6 °C. In double-pass mode, DPSAC-Se also outperformed DPSAC-Bl, with maximum absorber temperatures of 66.4 °C, 61.7 °C, 59.1 °C, and 57.1 °C, compared to 64.9 °C, 60.5 °C, 57.6 °C, and 55.8 °C at corresponding MFRs of 0.00877 kg/s, 0.01059 kg/s, 0.01425 kg/s, and 0.01632 kg/s, respectively. These results highlight the selective coating's effectiveness in enhancing thermal performance by increasing energy absorption and reducing heat loss. While single-pass collectors benefit from higher absorber temperatures, double-pass collectors maintain improved outlet temperatures and thermal efficiency, showcasing the coating's advantages in both configurations.

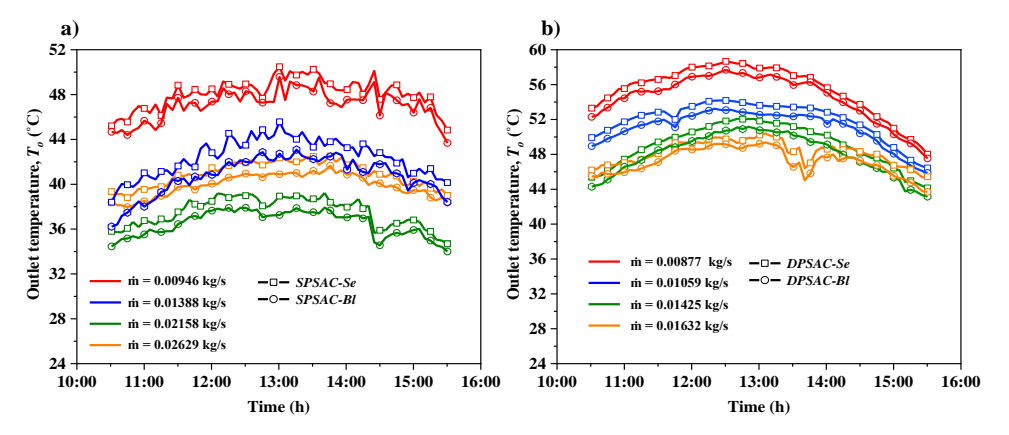


Fig. 11. Outlet temperature profiles for the collectors over time

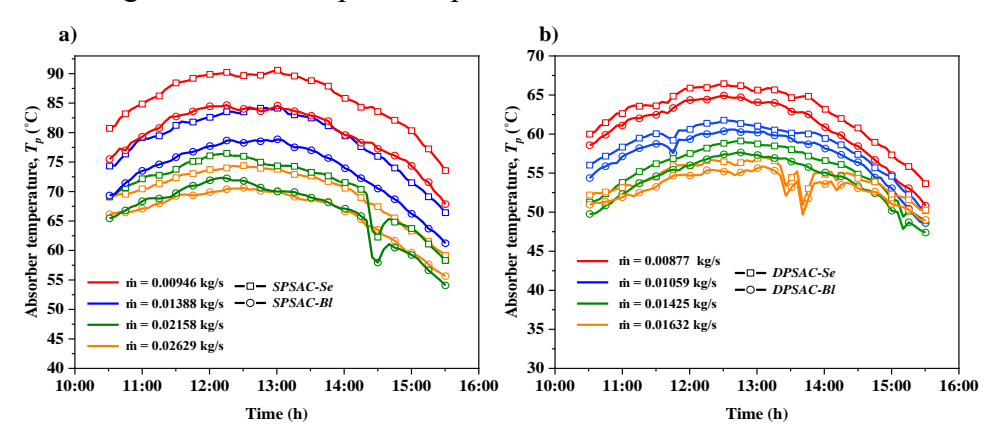


Fig. 12. Temperature variations of the absorbing plate over time

Fig. 13 a) highlights the difference in daily efficiencies between SPSAC-Bl and SPSAC-Se across various MFRs. Efficiency increases with MFR for both, but SPSAC-Se consistently outperforms SPSAC-Bl. At 0.00946 kg/s, SPSAC-Se achieves 39.2% efficiency compared to SPSAC-Bl's 37.1%, a 5.6% relative improvement. At higher MFRs, SPSAC-Se efficiencies reach 48.6%, 55.5%, and 66.2%, surpassing SPSAC-Bl by 10.9%, 9.0%, and 9.2%,

respectively. In double-pass mode (Fig. 13 b), DPSAC-Se also outperforms DPSAC-Bl, achieving efficiencies of 53.1%, 57.3%, 60.1%, and 63.0% at MFRs of 0.00877, 0.01059, 0.01425, and 0.01632 kg/s, compared to DPSAC-Bl's 51.4%, 55.3%, 56.7%, and 59.3%. This represents relative improvements of 3.3% to 6.2%. These findings underscore the superior performance of selective-coated collectors in both configurations, with relative enhancements ranging from 5.6% - 10.9% in single-pass mode and 3.3% - 6.2% in double-pass mode. The coating's ability to minimize radiative losses and enhance energy absorbing is more pronounced in single-pass mode due to higher absorber temperatures. In double-pass mode, lower absorber temperatures slightly reduce the coating's relative impact, but it remains effective in improving thermal performance.

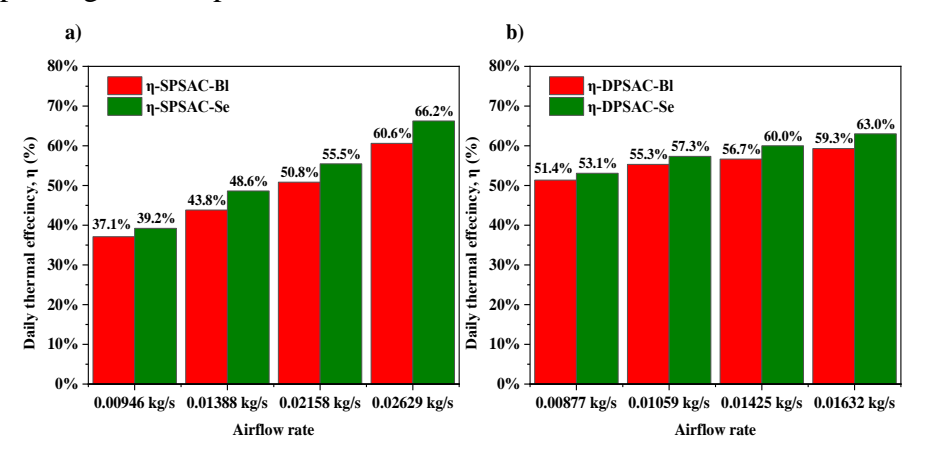


Fig. 13. The daily thermal efficiency versus airflow rate

3.4. Influence of channel depth evaluation

3.4.1. Effect on single pass mode

In August 2024, experiments evaluated single-pass collectors with varying channel depths. Two collectors were tested simultaneously: the reference SPSAC-5.5 cm with a 5.5 cm depth and a modified collector. Tests included SPSAC-7.5 cm (7.5 cm depth) and SPSAC-3.5 cm (3.5 cm depth), each at low and high flow rates. Consistent conditions ensured both collectors experienced identical ambient temperatures and solar radiation, isolating the effect of channel depth on performance. Fig. 14 shows outlet temperature profiles for varying MFRs and channel depths. Temperatures rise steadily in the morning, peak between 11:30 and 12:30, and decline in the afternoon as solar radiation decreases. Higher MFRs generally result in lower outlet temperatures for all configurations. At 0.00892 kg/s, SPSAC-3.5 cm reached 54.2 °C, slightly higher than SPSAC-5.5 cm's 52.9 °C, due to the shallower channel enabling more effective heat transfer through increased air velocity. At 0.01813 kg/s,

SPSAC-3.5 cm achieved 48.6 °C, compared to 47.7 °C for SPSAC-5.5 cm, with the difference diminishing as forced convection dominated. For SPSAC-5.5 cm and SPSAC-7.5 cm, maximum temperatures at 0.00901 kg/s were 49.1 °C and 48.3 °C, respectively, with SPSAC-5.5 cm maintaining a consistent advantage. At 0.01527 kg/s, SPSAC-5.5 cm recorded 50.2 °C, outperforming SPSAC-7.5 cm at 48.9 °C, indicating the optimal balance of air velocity and convective heat transfer in the 5.5 cm channel. The results highlight the importance of channel depth, particularly at lower flow rates, where shallow channels like SPSAC-3.5 cm enhance heat transfer. SPSAC-5.5 cm offers balanced performance across flow rates, while the deeper channel of SPSAC-7.5 cm retains heat but limits outlet temperatures at higher flow rates due to reduced residence time.

Fig. 15 shows daily efficiencies for tested collector at different MFRs.SPSAC-3.5cm collector outperforms SPSAC-5.5cm at 0.00892 kg/s and 0.01813 kg/s, achieving efficiencies of 37.6% and 56%, respectively, compared to 36% and 52.9% for SPSAC-5.5cm. The 4.4%–5.8% relative improvement is due to the shallower channel's faster airflow and enhanced convective heat transfer. SPSAC-5.5cm consistently outperforms SPSAC-7.5cm at 0.00901 kg/s and 0.01527 kg/s, with efficiencies of 38.5% and 52.6%, compared to 36.4% and 49.1% for SPSAC-7.5cm, reflecting 4.9%–7.1% relative gains. The deeper channel in SPSAC-7.5cm reduces convective heat transfer due to slower airflow. Optimizing channel depth is crucial for balancing efficiency and operational costs. While SPSAC-3.5cm offers higher efficiency, it increases pressure drops and pumping power. SPSAC-5.5cm provides a balanced solution, combining high efficiency with manageable energy costs, making it more versatile for diverse applications.

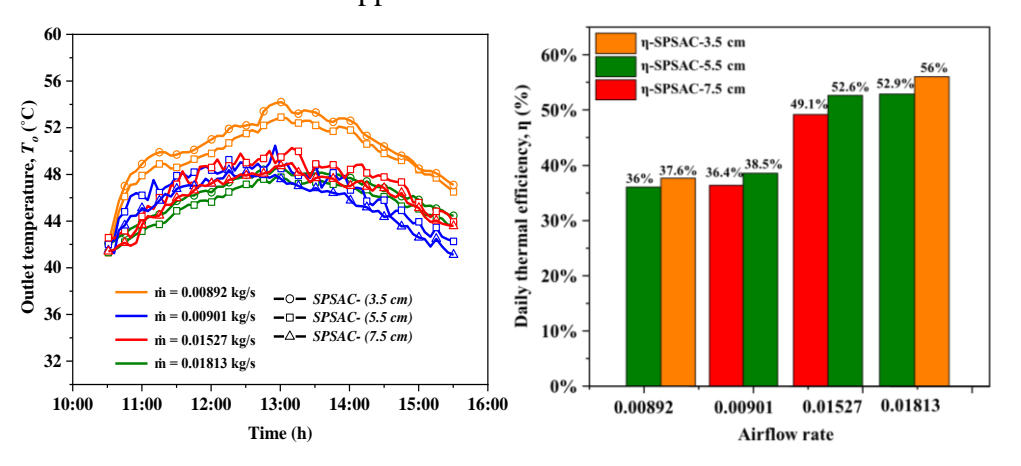


Fig. 14. Outlet temperature profiles for the collectors over time

Fig. 15. The daily thermal efficiency versus airflow rate

3.4.2. Effect on double pass mode

The effect of channel depth on DPSAC performance was analyzed using mathematical modeling. Validation experiments at a fixed 5.5 cm upper channel depth and 0.0103 kg/s mass flow rate showed strong agreement with the model, confirming its accuracy. The validated model was then used to assess the impact of varying upper channel depths on thermal efficiency, complementing the experimental results for single-pass collectors.

Fig. 16 compares predicted and experimental results for outlet temperature, demonstrating excellent agreement between the model and experimental data. The R^2 value for outlet temperature is 0.989, indicating the model accounts for 98.9% of the variability. These results confirm the model's high accuracy and reliability in predicting DPSAC performance under the tested conditions.

The derived equation at a MFR of 0.0103 kg/s were applied to the entire experimental dataset, capturing significant variations, as shown in Fig. 17. Additional validation using experimental data at flow rates of 0.0088, 0.0137, and 0.0143 kg/s yielded R^2 values ranging from 0.932 to 0.989 for outlet temperature, indicating strong correlations.

The model was then employed to simulate DPSAC performance across a range of channel depths (2.5 cm to 11.5 cm) and mass flow rates (0.0088 to 0.021 kg/s). The simulations revealed a distinct relationship between channel depth and mass flow rate in determining the thermal performance of DPSAC. At lower flow rates, shallow channels significantly enhance thermal performance, resulting in higher outlet temperatures and efficiencies due to improved heat transfer between the air and the absorber plate. The reduced channel depth increases air velocity, enhancing the convective heat transfer coefficient.

As flow rates increase, the influence of channel depth diminishes, and airflow becomes the dominant factor governing performance. Beyond a certain point, the benefits of varying channel depth are minimal, as forced convection takes precedence over the effect of channel geometry. This shift underscores the importance of optimizing both channel depth and flow rate for specific operational conditions.

In conclusion, the combined analysis of outlet temperature and thermal efficiency highlights the critical role of channel depth in SAC design. While shallow channels provide substantial performance improvements at low flow rates, moderate depths balance efficiency and airflow requirements, offering versatility across a range of applications. These simulation findings align closely with experimental results, reinforcing the understanding of how channel depth and mass flow rate interact to influence thermal performance in

SACs. By tailoring these parameters, maximum efficiency and thermal output can be achieved, ensuring optimal system performance

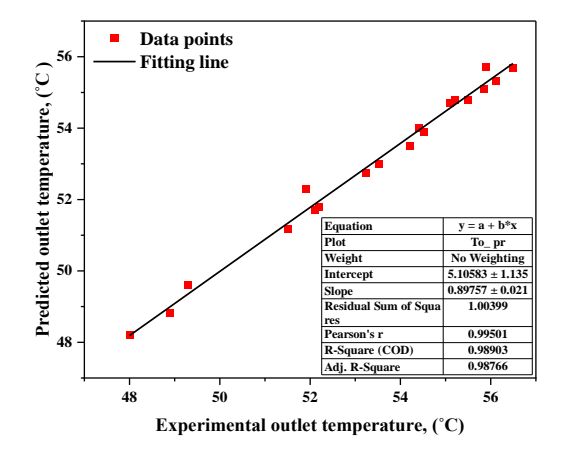


Fig. 16. Comparison of predicted and experimental data for outlet temperature

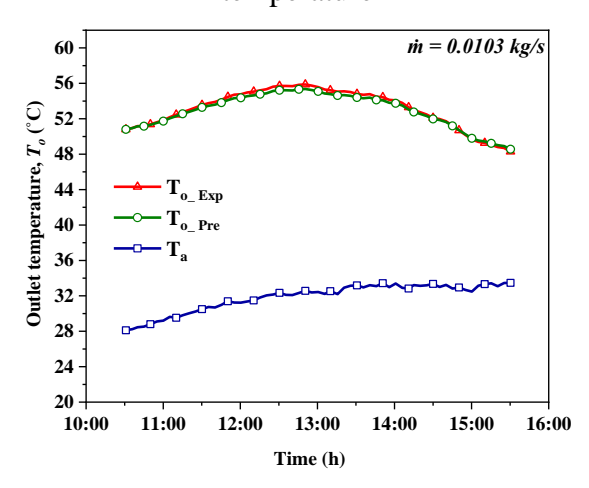


Fig. 17. Hourly variation of predicted and experimental data at 0.0103 kg/s

3.5. Effect of different fins configuration on drying process

This section presents the effect of fin shapes and orientations on drying efficiency in SACs during apple slice dehydration. Four configurations were tested: *Type I* (parallel fins), *Type II* (45° inclined fins), *Type III* (perpendicular fins), and *Type IV* (continuous V-angled fins). Tests were conducted over five hours, measuring outlet temperature, absorber plate temperature, airflow rates, humidity levels, and temperature variations inside the drying chamber. Two DPSACs were used: one with fins and the other with a smooth absorber as a control, each connected to dehydration chamber holding 1200 grams of apple slices. All tests were conducted under a single airflow rate and repeated for reliability, the tests provided direct comparisons

of drying rates, thermal efficiency, and temperature profiles, highlighting the impact of fin designs on performance.

Fig. 18 shows that dryers connected to FDPSAC consistently achieve higher drying efficiency than those with smooth collectors due to increased useful energy and higher drying chamber temperatures, accelerating moisture evaporation. The *Type I* achieves a drying efficiency of 20.7%, a 4% relative improvement over the smooth collector's 19.9%. *Type III* reaches 21.3%, outperforming the smooth collector's 19.4% by 9.7%. *Type III* shows a 20.5% efficiency compared to 19.2% for the smooth collector, a 6.7% relative increase. *Type IV* matches *Type II* with 20.9%, a 10.8% relative improvement over the smooth collector's 18.9%. These results demonstrate the significant role of fins in improving heat transfer and drying efficiency. Notably, *Types II* and *IV* exhibit the most substantial improvements, attributed to their enhanced collector performance. Further efficiency improvements may be achieved by increasing the airflow rate beyond the tested 0.0103 kg/s, warranting future investigations at higher flow rates.

Fig. 19 shows the initial and final weights of dried apple slices for each configuration, with all experiments starting at 1200 g. The FDPSAC consistently achieved lower final weights than the smooth collector, due to higher chamber temperatures and improved moisture evaporation. For *Type I*, the FDPSAC reduced the weight to 531 g (55.7% of the initial weight) compared to 557 g for the smooth collector, with a 4.7% relative improvement. *Type II* achieved 514 g (57.1%), outperforming the smooth collector's 572 g by 10.1%. *Type III* reduced the weight to 542 g (54.8%), a 7.4% relative improvement over the smooth collector's 585 g. *Type IV* achieved 548 g (54.3%), surpassing the smooth collector's 614 g by 10.7%.

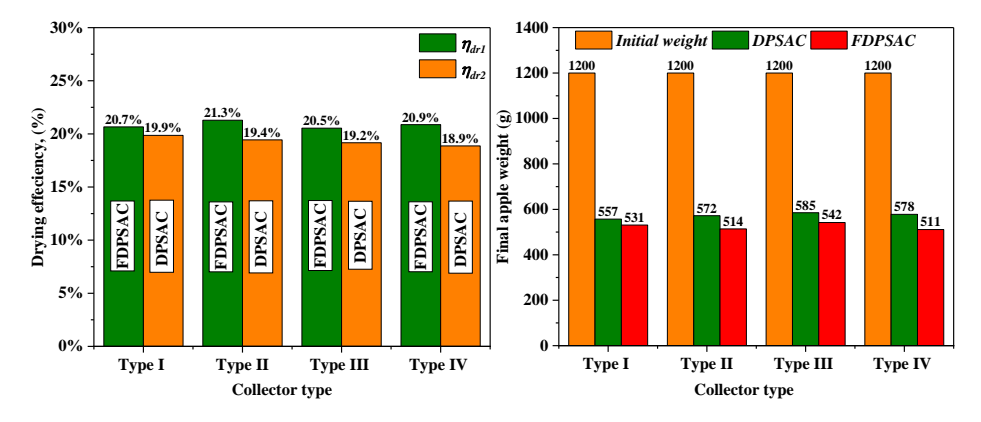


Fig. 18. The drying efficiency using proposed configurations

Fig. 19. The final weight of the dried apple using proposed configurations

4. NEW SCIENTIFIC RESULTS

This section presents the new scientific findings from the research work as follows:

1. Modification of entrance flue design

Based on experimental results, I evaluated and demonstrated the significant impact of entrance flue design on the thermal performance of solar air collectors. The entrance flue plays a crucial role in directing airflow into the collector, which directly influences heat transfer efficiency and overall performance. Additionally, the proposed entrance flue design enhances heat extraction by enhancing air distribution across the absorber plate, reducing dead zones, and resulting in lower absorber plate temperatures compared to the side entrance solar air collector (SAC). Through the proposed entrance design, a relative improvement in daily thermal efficiency, ranging between 6.9% and 7.4%, achieved solely by changing the air entrance from a side to a front configuration in the SPSAC.

Furthermore, I developed a linear model for the thermal efficiency of the front entrance single pass solar air collector, expressed as a function of the average fluid to ambient temperature difference and solar intensity:

$$\eta = a - b \frac{T_{f,av} - T_a}{I}$$

The model's coefficients of correlation for various flow rates are as follows:

$$\dot{m} = 0.01118 \text{ kg/s } [a = 0.450, b = 5.696, R^2 = 0.910]$$

$$\dot{m} = 0.01231 \text{ kg/s } [a = 0.516, b = 9.888, R^2 = 0.932]$$

$$\dot{m} = 0.01469 \text{ kg/s } [a = 0.601, b = 11.406, R^2 = 0.946]$$

2. Effect of the V- angled perforated fins

I have developed and evaluated novel V-angled perforated fins in both continuous and discrete configurations to enhance the thermal performance of double-pass solar air collectors (DPSAC). The proposed fins were tested in various orientations, with attachments on the upper absorber surface of the collector. The discrete V-angled perforated fins were arranged in three configurations: parallel to the flow (*Type II*), inclined at 45° to the flow (*Type III*), and perpendicular to the flow (*Type III*). In contrast, the continuous V-angled perforated fins were positioned perpendicular to the flow direction.

I have demonstrated that the daily thermal efficiency of the continuous V-angled fins achieved a relative improvement ranging from 4.5% to 9.8%, depending on the tested mass flow rate. This enhancement is attributed to the increased heat transfer area and the turbulence-generating effect of the fins,

which significantly improve heat transfer performance. Similarly, the discrete V-angled fins displayed efficiency improvements between 4.1% and 9.1%, with variation based on fin orientation and airflow rate.

Moreover, I have proved that fin orientation significantly influences the overall efficiency of DPSACs. *Type I* demonstrated the least enhancement, with relative improvements ranging from 4.1% to 5.1%. In contrast, *Type II* provided the most substantial enhancement, ranging from 5.9 % to 9.1%. *Type III* followed with relative efficiency gains between 4.3% and 5.9%. The finned collector surpasses the smooth collector in all configurations, regardless of the flow rates. These findings highlight the critical role of fin design and orientation in optimizing the thermal performance of SACs, making the V-angled fins a versatile solution applicable to various DPSAC designs.

3. Impact of selective coatings on collector performance

Based on experimental results, I have demonstrated that selective coatings significantly enhance the thermal performance of SACs by increasing energy absorption and reducing radiative heat losses. This enhancement is reflected in higher absorber plate temperatures and improved outlet temperatures compared to standard black matte coatings. The application of selective coatings also leads to notable improvements in thermal efficiency across different collector configurations and mass flow rates. A relative improvement in thermal efficiency has been observed, with increases ranging from 5.6% to 10.9% in SPSACs and from 3.3% to 6.2% in DPSACs, depending on the tested mass flow rate. These efficiency gains underscore the coating's role in improving energy absorbing and retention. Moreover, the experimental findings, revealed that selective coating has a considerably stronger effect on the SPSAC compared to the DPSAC, this due to differences in airflow dynamics and heat transfer mechanisms between the two collectors.

To further interpret these findings, I have developed a quadratic regression model to predict the absorber plate temperature as a function of solar radiation intensity, mass flow rate. This model is applicable within a solar radiation range of $600-1000~\rm W/m^2$ and mass flow rates from 0.00877 to $0.02629~\rm kg/s$ for both selective and non-selective coatings. It provides a reliable method for predicting the absorber plate temperature in various solar collector designs under varying conditions. The general form of the model is:

$$\hat{T}_{v} = \boldsymbol{a} \cdot \boldsymbol{I} + \boldsymbol{b} \cdot \dot{m} + \boldsymbol{a}_{2} \cdot \boldsymbol{I}^{2} + \boldsymbol{b}_{2} \cdot \dot{m}^{2} + \boldsymbol{d} \cdot \boldsymbol{I} \cdot \dot{m} + \boldsymbol{c}$$

SPSAC-Se [a= 0.0436, b= -3691.7, $a_2 = 5.22 \times 10^{-7}$, $b_2 = 82244.8$, d = -0.1167, c = 76.22 R²=0.969] SPSAC-Bl [a= 0.0373, b= -3340.4, $a_2 = 4.55 \times 10^{-6}$, $b_2 = 74108.9$, d = -0.0949, c = 69.96, R²=0.974] DPSAC-Se [a= 0.0794, b= -6050.2, $a_2 = -1.572 \times 10^{-5}$, $b_2 = 2.837 \times 10^{5}$, d = -2.4853, c = 56.16, R²=0.941] DPSAC-Bl [a= 0.0938, b= -4498.1, $a_2 = -1.958 \times 10^{-5}$, $b_2 = 2.429 \times 10^{5}$, d = -3.0049, c = 38.26 R²=0.946]

4. Influence of channel depth on collector performance

Based on experimental and modelling results, I evaluated how channel depth affects the thermal performance of both single-pass and double-pass solar air collectors. Channel depth significantly influences airflow patterns and heat transfer efficiency within the collector. Shallow channels enhance heat transfer but increase flow resistance, demanding more power to maintain airflow, whereas deeper channels reduce resistance but sacrifice thermal performance.

For single-pass collectors, I have demonstrated that shallow channel depth improved daily efficiency by 4.4% at a low flow rate and by 5.8% at a higher flow rate compared to the moderate depth. In comparison, the moderate depth outperformed the deepest channel at both low and higher flow rates, showing efficiency gains improvements of 4.9% and 7.1%, respectively. These results underscore that a shallower channel enhances efficiency at low flow rates, while a moderate depth provides balanced performance across conditions, optimizing efficiency.

In double-pass collectors, I have developed a MATLAB-based mathematical model to predict the outlet temperature with high accuracy, achieving an R² value of 0.989. This model was validated through experiments and used for simulating the effect of varying upper channel depths on collector performance. Based on simulation results, I have demonstrated that at low flow rates, shallow upper channels substantially improve thermal efficiency due to enhanced heat transfer. Moreover, at high flow rates, the impact of channel depth decreases as air velocity becomes the dominant factor in heat transfer, resulting in stable efficiency across different channel depths.

Furthermore, selecting a moderate channel depth minimizes pressure drop and reduces the need for additional pumping power, enhancing system performance in both single-pass and double-pass collectors. This balanced approach ensures optimal thermal efficiency while maintaining energy-efficient operation, making it applicable to various solar air collector design.

5. Comparison of different fin configurations on drying performance

I have proved that the configuration of fins significantly influences drying performance within the DPSAC, as shown by variations in drying efficiency and final product weight across different fin arrangements. The experiments revealed that continuous V-angled fins *Type IV*, oriented perpendicular to the airflow, deliver the highest enhancement in performance, with a 10.8% improvement in drying efficiency compared to the smooth collector. Additionally, the discrete V-angled *Type II* fins demonstrated strong

4. New scientific results

performance, increasing drying efficiency by 9.7% relative to the smooth collector.

I found that fin orientation significantly affects the drying efficiency of solar air collectors. Fins oriented parallel to the airflow (*Type I*) and those positioned perpendicular to the airflow (*Type III*) demonstrated moderate improvements in drying efficiency and final product weight compared to the smooth collector. In contrast, *Type II* fins, inclined at 45°, achieved a drying efficiency of 21.3%, surpassing the 19.4% efficiency of the smooth collector, thus reflecting a relative increase of 9.7%.

5. CONCLUSION AND SUGGESTIONS

An experimental analysis of design enhancements was conducted to improve SAC thermal performance. For single-pass collectors, testing front versus side entrance configurations showed that the front entrance significantly improved airflow distribution and heat transfer, resulting in efficiency gains between 6.9% and 7.4%. In double-pass SACs, continuous and discrete V-angled fins were evaluated. Continuous fins, oriented perpendicular to airflow, improved efficiency by 4.4% to 9.8%, depending on mass flow rate. Among discrete fins, those inclined at 45° to the airflow achieved the highest thermal performance, with gains of 4.1% to 9.1% based on configuration and flow rate.

Selective coatings applied to absorber plates yielded notable efficiency improvements. In single-pass collectors, efficiency increased by 5.6% to 10.9%, while double-pass collectors showed gains of 3.3% to 6.2%. These improvements were attributed to enhanced solar absorbing, reduced radiative losses, and increased absorber plate temperatures, leading to more consistent outlet air temperatures, especially under fluctuating solar conditions. Channel depth analysis revealed that shallow channels improved heat transfer at low flow rates, while moderate channel depths offered a balance between efficiency and reduced pressure drops, making them suitable for varying operating conditions.

In drying applications, the influence of fin orientation on drying efficiency was assessed using apple slices. Continuous V-angled fins oriented perpendicular to airflow increased drying efficiency by 10.8%, while discrete fins inclined at 45° achieved a 9.7% improvement. These configurations maintained higher drying temperatures, accelerated moisture removal, and reduced drying times, enhancing the drying process.

Future work should explore the effects of friction and pressure drops in collectors, as these factors impact system efficiency. Further optimization of fin configurations, such as fin angles, perforation patterns, and spacing, could maximize thermal performance and airflow in double-pass SACs. Additionally, investigating environmental factors like solar radiation, ambient temperature, and humidity would provide insights into finned SAC performance under diverse conditions.

The integration of selective coatings with phase change materials (PCMs) could further enhance SAC energy storage by improving solar absorption and reducing PCM charging time. Such advancements, coupled with optimized designs, could lead to highly efficient solar collectors adaptable for thermal energy capture and agricultural drying applications.

6. SUMMARY

EFFICIENCY IMPROVEMENT OF SOLAR AIR COLLECTORS USED IN DRYING PROCESSES

A detailed experimental study was conducted in Gödöllő, Hungary, to enhance the efficiency of solar air collectors (SACs) for drying applications. The research, carried out at the Solar Energy Laboratory of the Hungarian University of Agriculture and Life Sciences (MATE), focused on improving thermal performance through modifications in entrance flue designs, fin configurations, selective coatings, and channel depths for both single-pass (SPSAC) and double-pass (DPSAC) systems.

For SPSACs, a front entrance flue was compared to a side entrance design. The results showed a 6.9–7.4% improvement in thermal efficiency for the front entrance due to better airflow distribution and heat transfer across the absorber plate. In DPSACs, discrete V-angled fins were tested in three orientations: parallel to airflow (*Type II*), inclined at 45° (*Type III*), and perpendicular to airflow (*Type III*). *Type II* fins achieved the highest efficiency gains, ranging from 5.9% to 9.1%, followed by *Type III* fins with gains of 4.3–5.9%, and Type I fins with gains of 4.1–5.1%. Continuous V-angled fins, oriented perpendicular to airflow, showed efficiency improvements of 4.5%–9.8%, further demonstrating the effectiveness of airflow disruption in enhancing heat transfer across varying flow rates.

Selective coatings applied to absorber plates resulted in significant thermal efficiency gains. In SPSACs, the improvement ranged from 5.6% to 10.9%, while DPSACs showed increases of 3.3–6.2%. These gains were attributed to the coatings' ability to enhance energy absorption and reduce radiative losses, leading to higher absorber plate temperatures and more consistent outlet air temperatures. Channel depth experiments revealed that shallower channels improved thermal performance at low flow rates by enhancing heat transfer, while moderate depths provided a balance between efficiency and reduced pressure drops, minimizing the need for additional pumping power.

Drying experiments used apple slices to evaluate drying efficiency under different fin configurations. Continuous V-angled fins oriented perpendicular to airflow achieved the highest efficiency improvement, with a 10.8% gain compared to smooth absorbers. Among discrete fins, the 45° inclined orientation (*Type II*) improved drying efficiency by 9.7%, highlighting its ability to disrupt airflow effectively. Parallel (*Type I*) and perpendicular (*Type III*) orientations also enhanced drying efficiency, though to a lesser extent than the 45° inclined fins. These findings underscore the importance of fin orientation in optimizing drying rates and thermal performance for agricultural applications.

- 7. MOST IMPORTANT PUBLICATIONS RELATED TO THE THESIS Refereed papers in foreign languages:
- 1. **Machi, M.H**, Buzas, J., Farkas I. (2020): Potential of solar energy utilization in Iraq, Mechanical Engineering Letters, Vol. 20, pp. 80–88. https://www.gek.szie.hu/english/sites/default/files/MEL_2020_20.pdf
- 2. **Machi, M.H.**, Al-Neama, M.A., Buzás, J., Farkas, I. (2022): Energy-based performance analysis of a double pass solar air collector integrated to triangular shaped fins, International Journal of Energy and Environmental Engineering, 13(1), pp. 219–229_{DOI}: 10.1007/s40095-021-00422-z DOI: 10.1007/s40095-021(664223; Q2, IF = 1.9)
 - 3. **Machi, M.H.**, Farkas, I., Buzas, J. (2024): Enhancing solar air collector performance through optimized entrance flue design: A comparative study, International Journal of Thermofluids, 21(January), Paper No. 100561. DOI: 10.1016/j.ijft.2024.100561 (Scopus: D1)
 - 4. **Machi, M.H.**, Farkas, I., Buzas, J. (2024): Enhancing thermal efficiency of double-pass solar air collectors: A comparative study on the role of V-angled perforated fins, Energy Reports, 12(December), pp. 481–494. DOI: 10.1016/j.egyr.2024.06.048 (Scopus: Q2, IF = 4.7)
 - 5. **Machi, M.H.**, Farkas, I., Buzas, J. (2025): Modelling the performance of double pass solar air collectors, European Journal of Energy Research, Vol. 5, No. 1, pp. 1-9. DOI: 10.24018/ejenergy.2025.5.1.159
 - 6. **Machi, M.H.**, Farkas, I., Buzas, J. (2025): Optimizing double-pass solar air collector efficiency: Impact of a perforated discrete V-angled fins, Energy Reports, Vol. 13, pp. 2021–2034. https://doi.org/10.1016/j.egyr.2025.01.057. (Scopus: Q2, IF = 4.7)
 - 7. **Machi, M.H.**, Zhu, Q.K., Farkas, I., Buzas, J. (2025): Impact of fin shape and orientation on drying performance in solar air collectors. Acta Technologica Agriculturae, xx(xx), pp. xxx-xxx. https://doi.org/xxxxxxxxxxxxxx. (IF = 1.3) (in progress)
 - 8. **Machi, M.H.**, Farkas, I., Buzas, J. (2025): Investigating the role of air channel depth on solar air collector performance. International Journal of Thermofluids, xx(xx), pp. xxx-xxx. https://doi.org/xxxxx/xxxxxx (Scopus: D1) (in progress)
 - 9. **Machi, M.H.**, Farkas, I., Buzas, J. (2025): Impact of selective coatings on efficiency of solar air collectors: An experimental investigation. Results in Engineering, xx(xx), pp. xxx-xxx. https://doi.org/xxxxx/xxxxxx (Scopus: Q1, IF = 6) (in progress)